



OPEN ACCESS

EDITED BY

Hu Li,
Southwest Petroleum University, China

REVIEWED BY

Dianshi Xiao,
China University of Petroleum, Huadong,
China
Xixin Wang,
Yangtze University, China
Huafeng Tang,
Jilin University, China

*CORRESPONDENCE

Qingyou Yue,
✉ yueqingyou@lnpu.edu.cn

RECEIVED 09 March 2023

ACCEPTED 14 April 2023

PUBLISHED 09 May 2023

CITATION

Yue Q, Wang B, Ren X, Cang Z, Han J, Li C,
Zhao R and Wang H (2023), Classification,
identification, and reservoir
characteristics of intermediate mafic lava
flows: a case study in Dongling area,
Songliao Basin.

Front. Earth Sci. 11:1182711.

doi: 10.3389/feart.2023.1182711

COPYRIGHT

© 2023 Yue, Wang, Ren, Cang, Han, Li,
Zhao and Wang. This is an open-access
article distributed under the terms of the
[Creative Commons Attribution License
\(CC BY\)](https://creativecommons.org/licenses/by/4.0/). The use, distribution or
reproduction in other forums is
permitted, provided the original author(s)
and the copyright owner(s) are credited
and that the original publication in this
journal is cited, in accordance with
accepted academic practice. No use,
distribution or reproduction is permitted
which does not comply with these terms.

Classification, identification, and reservoir characteristics of intermediate mafic lava flows: a case study in Dongling area, Songliao Basin

Qingyou Yue^{1*}, Baozhu Wang¹, Xianjun Ren², Zhengyi Cang³,
Jiaoyan Han², Cunlei Li¹, Ranlei Zhao¹ and Haidong Wang¹

¹College of Petroleum and Natural Gas Engineering, Liaoning Petrochemical University, Fushun, China, ²Northeast Oil & Gas Branch of Sinopec, Changchun, China, ³Chengdu Exploration and Development Research Institute, Petro China Daqing Oilfield Company LTD, Chengdu, China

Intermediate mafic lava is a special oil and gas reservoir. While its internal structure is an important factor affecting the reservoir properties, the identification of facies and understanding of the relationship between facies architecture and reservoir are limited. This study evaluated the intermediate mafic lava flows of the Yingcheng Formation in the Dongling area of Songliao Basin by analyzing the drilling cores, corresponding thin sections, and scanning electron microscope (SEM) images, as well as well-logging and seismic attributes. We also performed helium gas experiments and high-pressure mercury intrusion (HPMI) analysis to assess the physical properties and pore structure of the reservoir, respectively. The results showed that intermediate mafic lava flows develop tabular lava flow, compound lava flow, and hyaloclastite. Three facies showed present diverse well-logging and seismic responses. The intermediate mafic lava facies architecture was divided into crater-proximal facies (CF-PF), medial facies (MF), and distal facies (DF), which were characterized by their vesicles and joints and could be identified through their seismic attributes. The reservoir spaces including vesicles, amygdale inner pores, joint fissures, and dissolution pores predominantly showed oil and gas accumulation. The results of the tests of the reservoir's physical properties showed that the reservoir quality was best in the CF-PF, which is the main target of oil and gas exploration.

KEYWORDS

intermediate mafic lava flows, Dongling area, Yingcheng Formation, facies architecture, reservoir characteristics

1 Introduction

Volcanic reservoirs are widely distributed in many basins worldwide and have been the target of oil and gas exploration and development for more than 130 years (Zou et al., 2008). A small number of volcanic reservoirs are composed of acidic volcanic rocks, such as the Yo-shii Kashiwazaki rhyolite gas field in Niigata Basin in Japan (Zhao et al., 2009). Most volcanic reservoirs are dominated by intermediate mafic volcanic rocks, such as basalt in the Scott Reef oil fields and the gas fields in Australia; basalt and basaltic agglomerates in the West Rozel oil field in North Basin, USA; and vesicle basalt in the YPF Palmar Largo oil field in Noro Este Basin, Argentina (Passey et al., 2007). Since the discovery of basaltic oil and gas reservoirs in the

northwestern margin of the Junggar Basin in 1957, volcanic oil and gas reservoirs in China have become the focus of comprehensive exploration (Zhao et al., 2009). The lithology of volcanic reservoirs differs between the eastern and western basins of China. The western basin is mainly composed of intermediate mafic volcanic rocks, while the eastern basin is acidic volcanic rocks (Hou et al., 2013). The intermediate mafic volcanic reservoirs in the western basins are mostly secondarily weathered or composed of volcanic pyroclastic rocks (Hou et al., 2003; Wang et al., 2011; Fan et al., 2020). With the increasing development of volcanic oil and gas fields in Songliao Basin, outcrop surveys and drilling have confirmed that the intermediate mafic reservoirs developed in the Early Cretaceous Yingcheng Formation in Songliao Basin (Huang et al., 2010; Shan et al., 2012; Zhang et al., 2018). Different from the western basin, the intermediate mafic lava reservoir is buried *in situ* with weak secondary reformation, making it a good material for the study of intermediate mafic lava flow structure and reservoir characteristics.

Intermediate mafic lava flows with vast extent and emplacement on low slopes are consistent with an eruption from point sources or along fissures (Walker et al., 1993; Marsh et al., 2001). The range of lava flows is wide and multiple eruption units overlap. For example, the basalt lava flows in the Faroe Islands extend at least 6.6 km (Self et al., 2013; Yi et al., 2016), and three different types of basalt flows (tabular, compound, and hyaloclastite) display a range of facies onshore (Greeley et al., 1982; Nelson et al., 2009). According to the maximum average slope, the volcanic basalt lava seismic facies are divided into three types: mounded seismic facies units (MSFUs), tabular seismic facies units (TSFUs), and mounded-tabular seismic facies units (M-TSFUs) (Tang et al., 2023). Based on petrographic studies of Mesozoic intermediate mafic volcanic rocks, Cenozoic Changbaishan basalt, and Wudalianchi basalt encountered in Songliao Basin, the intermediate mafic lava flows can be divided into braided, tabular, and fan lava flows (Wang et al., 2018). Significant progress has also been made in the study of the diagenesis and reservoir characteristics of intermediate mafic lavas (Huang et al., 2010; Liu et al., 2010; Ren et al., 2015). Previous studies based on thin section observations, SEM, MIP, and low-temperature nitrogen adsorption (LTNA) revealed the pore structure characteristics of intermediate mafic volcanic reservoirs (Cang et al., 2021). The internal structure of oil reservoirs has mostly focused on tight sandstone and shale reservoirs (Li et al., 2019; 2020; Shan et al., 2021; Li et al., 2023). Previous studies showed that the primary vesicles and fractures of intermediate mafic lava flows can form high-quality reservoirs for oil and gas migration and storage (Liu et al., 2010; Yue et al., 2021). However, several studies have reported the inner structure of intermediate mafic lava flows corresponds to the geophysical method.

Therefore, taking the intermediate mafic lava flows of the Yingcheng Formation in the Dongling region as an example, this study classified the types of lava flows by field outcrop observation and identified them based on the combination of drilling cores, logging curves, and 3D seismic profiles. The reservoir space types of different lava flows were observed by casting thin sections and SEM, and the micropore structure was analyzed by HPML. In addition, the reservoir properties and pore structure of different lava flows were clarified. Combined with the analysis of reservoir space type and diagenesis, we established a reservoir geological model of intermediate mafic lava flows. This study has a practical significance for recognizing the distribution of intermediate mafic lava flow reservoirs.

2 Geological setting and samples

2.1 Geological setting

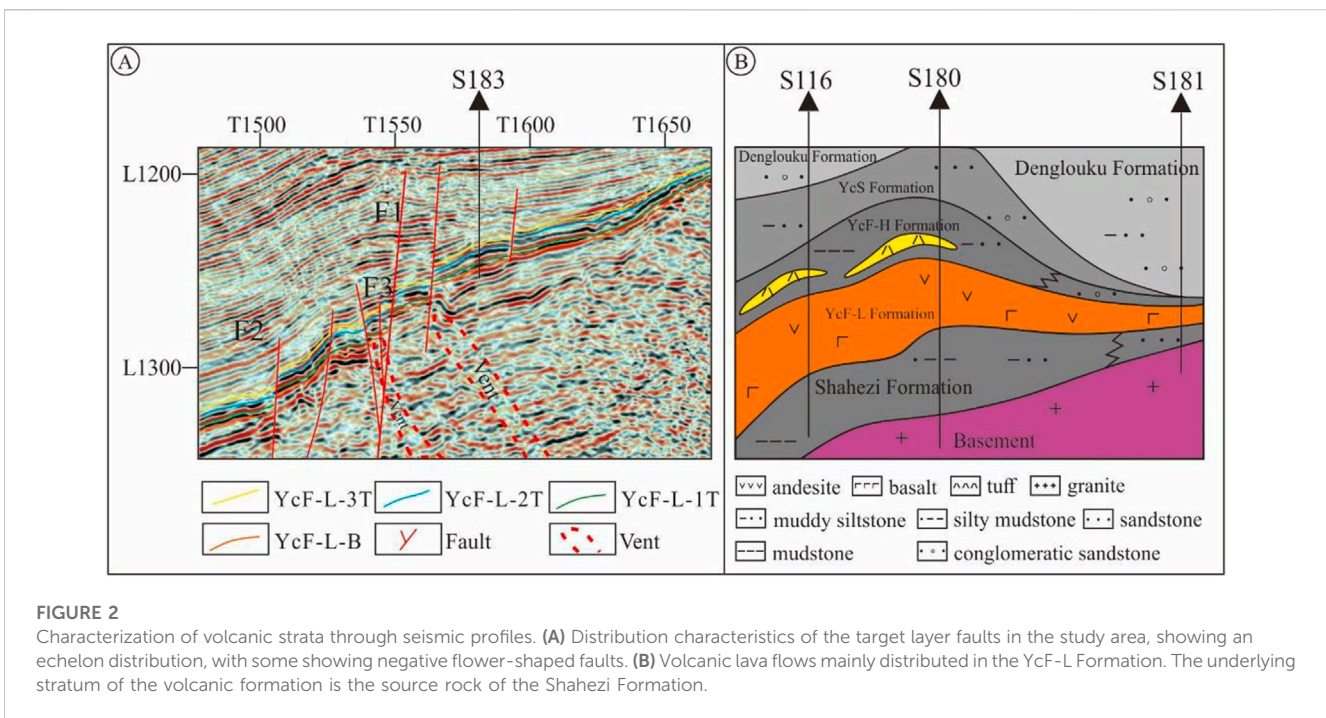
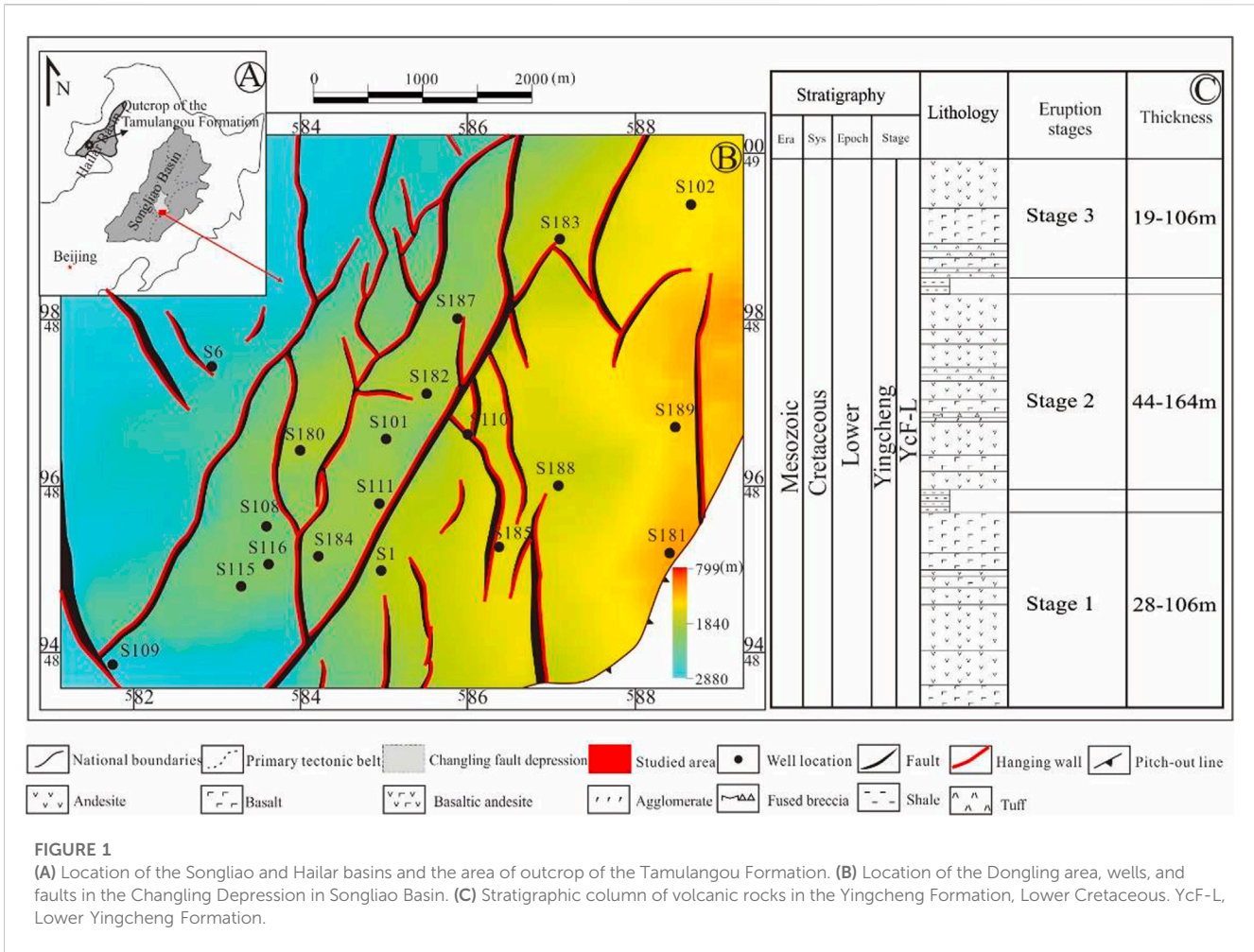
The study region (Figures 1A, B) is located in the southern part of the Changling fault depression of Songliao Basin, controlled by a series of NNE- or NE-trending basement fractures under the consumption effect of ocean-continent subduction in the Mesozoic (Ren et al., 2002; Wei et al., 2010; Feng et al., 2014). Fault activity controls the development of the fault depression and volcanic eruption intensity. The fault development scale is different and can be divided into three levels, F1, F2, and F3 (Figure 2). The F1 faults run from south to north, extending up to 16 km, with large fault distances, and control the development of the fault depression. The F2 fault is the secondary fault, with a smaller scale and extension than those of F1, and generally 20–50 m between faults. The F3 fault is the branch fault of F1 and F2, with a small fault distance and short extension, which develops in a nearly north-south direction. The faults are distributed in an echelon from west to east, and the section shows a negative flower structure. The strata on the lower side of the fault are fully developed and thick, while those on the upper side gradually become thinner, with some missing strata.

Large-scale volcanic eruptions occurred in Songliao Basin during the Late Jurassic-Early Cretaceous Period (Figure 2). The strata from bottom to top are the Huoshiling Formation, Shahezi Formation, and Yingcheng Formation, respectively (Tang et al., 2008; Wang et al., 2015). The study region experienced extension during the Huoshiling stage, along with volcanic and continental deposits. During the Shahezi stage, the strata continued to be subjected to the east-west tension, and the water body gradually became deeper so that the sedimentary environment evolved from a shore-shallow lake to a deep lake (Zhang et al., 2012). As a result, it provides a good oil and gas supply for the Yingcheng Formation volcanic reservoirs. Based on 19 wells penetrating the volcanic rocks of the Yingcheng Formation, the maximum thickness of lava flows in the Yingcheng Formation is >400 m. The first member of the Yingcheng Formation consists of the main lava flows that are primarily composed of basalt, basaltic andesite, and a thin layer of pyroclastic rocks. These can be divided into three eruption stages according to the thick deposition layers, which are mainly gray and black shale (Figure 1C).

2.2 Samples and methods

A total of 12 representative core samples were collected from six wells in the study region, including basalt, basaltic andesite, and trachybasalt. Among them, the lava samples contained vesicle lava and dense lava. The samples represented the characteristics of different lava flows, and core sample pictures are shown in Figure 3. The porosity and permeability data were obtained by helium gas assessments of the high-pressure physical properties. Information on the rock samples including well, depth, lithology, and physical properties is shown in Table 1.

The samples were cut into standard cylinders (3 cm in length, 2.54 cm in diameter). After washing and drying, helium gas



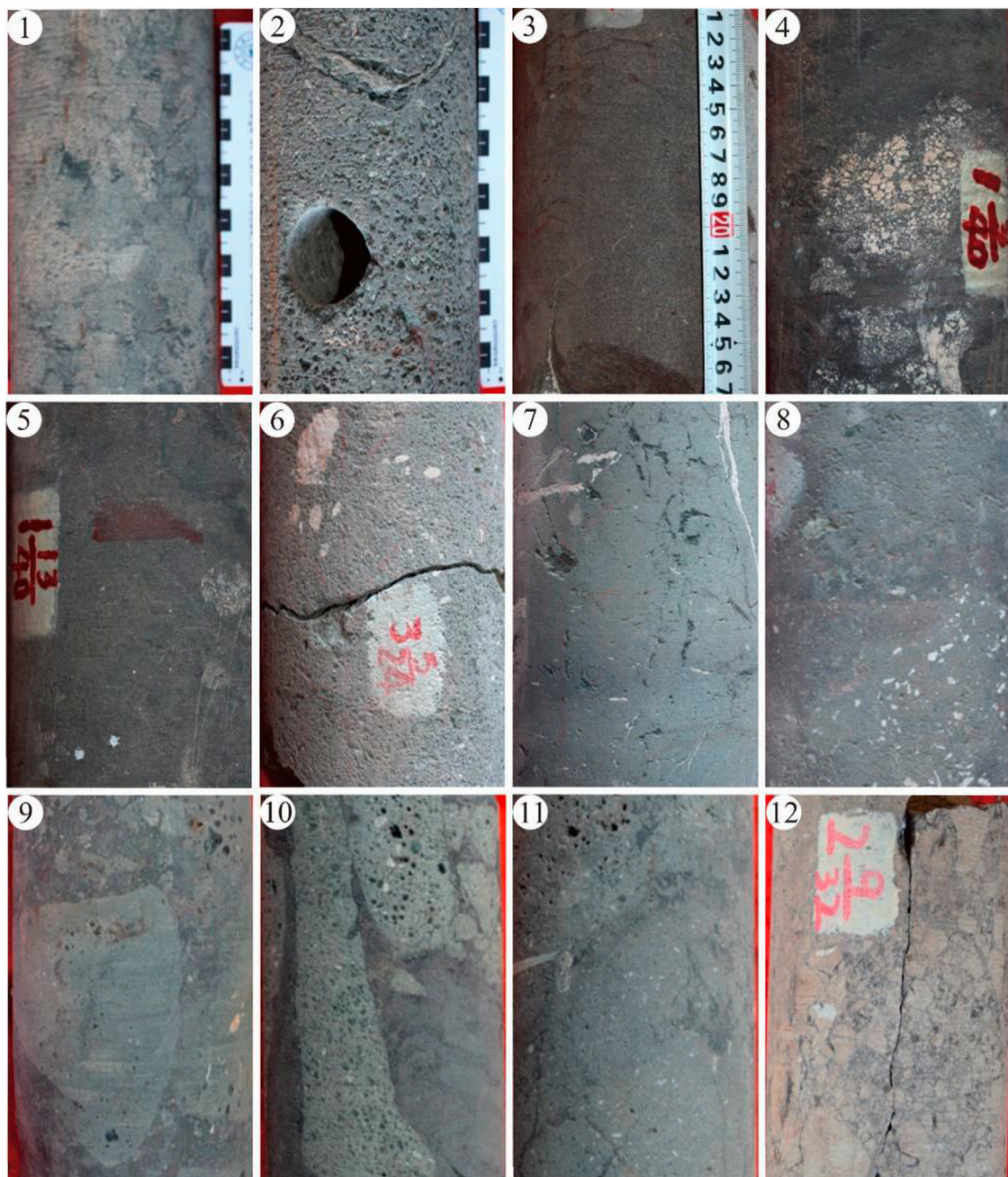


FIGURE 3

Pictures of 12 volcanic core samples obtained from the Yingcheng Formation. All core samples are full-hole cores from six wells.

experiments, casting thin sections, SEM, and HPMT experiments were performed successively. The helium gas experiments, casting thin sections, and SEM were carried out at the Laboratory at Jilin University. The HPMT experiments were performed on a Pore Master-60 GT at the Beijing Center for Physical and Chemical Analysis, according to the National Standard GB/T 21650.1. The pore size range of the HPMT was >9 nm, which can be used to characterize the pore structure of the samples. In addition, basalt field outcrop profiles, seismic data, and well logging data in the study

region were obtained from Sinopec Northeast Oil and Gas Branch.

3 Results

3.1 Intermediate mafic lava flows in outcrops

Based on the observations of the basalt outcrop, including morphology, dimension, and internal structure in the middle

TABLE 1 Wells, depths, lithology, porosity, and permeability of 12 rock samples.

Sample	Well	Depth (m)	Lithology	Porosity (%)	Permeability (mD)
1	S1	2,402.2	Andesite	5.6	0.37
2	S1	2,408.2	Trachybasalt	9.9	0.5
3	S102	1857.1	Basalt	5.9	0.87
4	S116	2,709.7	Basalt	13.2	1.2
5	S116	2,711.7	Basalt	4.3	0.1
6	S187	2,432.9	Basaltic andesite	10.7	0.5
7	S187	2,453.3	Basaltic andesite	8.1	0.3
8	S187	2,436.1	Basalt	8.1	0.7
9	S180	2,480.2	Basaltic agglomerated lava	9.7	3.8
10	S180	2,471.5	Basaltic andesite	8.9	1.2
11	S180	2,472.9	Basaltic andesite	4.2	0.3
12	S183	1,986.6	Trachyandesite	12.8	2.56

Jurassic Tamulangou Formation at Hulun Lake in Inner Mongolia, the intermediate mafic lava flows at the Hailer Basin margin (Figure 1) can be divided into three representative lava flow units, including tabular lava flow, compound lava flow, and hyaloclastite.

The external shape of the tabular lava flows was similar to plate-like, with overlapping layers and large single-layer thickness, up to several tens of meters, with the extension of good continuity reaching several kilometers (Byrnes et al., 2002; Hachimi et al., 2010). It mainly formed in the phase of powerful volcano eruption and is the largest accumulation of the intermediate mafic lava flows (Figure 4A). A mass of primary pores of large size developed at the top of the tabular lava flows, while the bottom is mostly residual pores. The middle part shows a dense massive structure and columnar joints (Figure 4B).

The flow lobe of the compound lava flows is thin, similar to the braided channel. It is also interlaced overlapped and has a lineoid section (Figure 4A). Individual flow lobes comprise a lower crust, a core, and an upper vesicle belt. The core is compact with irregular jointing (Figure 4B). Compound lava flow often presents multiple layers of flow lobes in different volcanoes.

Hyaloclastite is common in the initial formation of underwater volcanic eruptions (Clague et al., 2013). After volcanic eruptions, the subaerial lava flow is quenched by water at the distal facies of the facies architecture (Caroff et al., 2019; Angulo et al., 2021). The hyaloclastite structure shows a glassy texture and broken breccia structure. When the lava flow encounters quenching condensation on the water, the internal lava maintains a higher temperature (Nichols et al., 2012). Under the influence of external temperature and pressure differences, the internal lava extrudes and condenses, forming a new condensation crust. Thus, the hyaloclastite is generally pillow-shaped (Figure 4A). The hyaloclastite has radioactive joints, and

the vesicles are mostly developed in the outer ring zone (Figure 4B).

3.2 Geophysical identification of lava flows

Intermediate mafic lava flows are distributed on the surface in shield-like or sheet-like shapes, with weak eruption intensity, and are generally formed by overflowing fissures (Walker et al., 1993; Single et al., 2004). Field geological surveys of volcanic architecture in Songliao Basin divided the volcanic institutions horizontally into CF-PF, PF, and DF (Wang et al., 2015). Wells S180, S183, and S1 in the study area revealed CF-PF, MF, and DF, respectively (Figures 5A–C). The CF-PF is mainly dominated by thick tabular lava, and compound lava flows are formed in the early stage of magma eruption. Hyaloclastite can form at the bottom of lava flows if the crater is in a lacustrine environment. The MF and DF are mainly composed of thin tabular and compound lava, respectively. The lava flows were quenched with water to form hyaloclastite.

The seismic reflection pattern of tabular lava is similar to sedimentary strata with parallel or subparallel features, characterized by strong amplitude and high frequency due to the dense block structure (Figure 5). The compound lava was a braided shape, with a medium frequency, medium amplitude, and subparallel type. The thin compound lava flows overlapped; thus, it was difficult to discern single lava lobes on the seismic sections. There are two forms of hyaloclastite formation; namely, when the lava flow overflows from the crater into the lake, in which the seismic reflection is characterized by a forest filling, and underwater volcanic eruption, in which the lava flow is quenched to form mushroom- or pillow-like structures. The internal seismic reflection is characterized by low frequency and weak amplitude.

Well-logging can represent the physical properties of different lava flows and their internal structural characteristics (Figure 5). Tabular lava showed high resistivity (LLD and LLS) in the range of

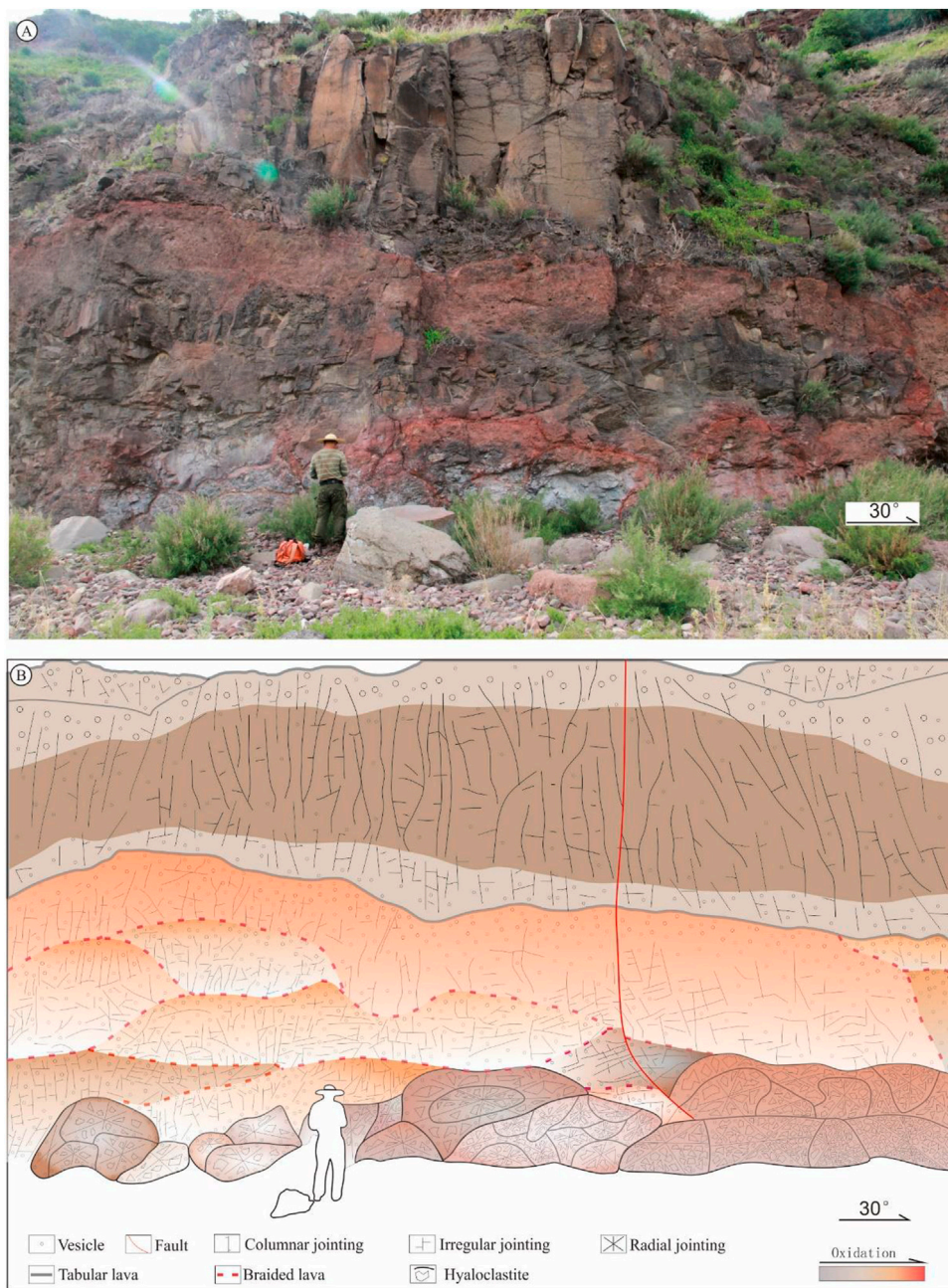


FIGURE 4
(A) Geological profile of lava flows in the upper Jurassic Tamulangou Formation of Hulun Lake, Inner Mongolia. **(B)** Sketch of different facies of intermediate mafic lava flows with corresponding vesicle, jointing, and geological morphology.

22 to 508 $\Omega \bullet m$ (average 268 $\Omega \bullet m$), high density (DEN) from 2.5 to 2.9 g/cm^3 , low acoustic (AC) from 190 to 272 $\mu s/m$, and showed box-shape. The resistivity at the top of the tabular lava was generally lower than other portions due to the pore development. The resistivity of the compound lava flow was generally smaller than that of the tabular lava flow, with a range of 10–100 $\Omega \bullet m$, AC 210–270 $\mu s/m$, and DEN is 2.3–2.7 g/cm^3 . The compound lava flow was characterized by interlaced overlapping thin-layer lava flows, with much smaller scales of pore and dense zones. The curves showed obvious finger shapes. The hyaloclastite showed lower LLD

or LLS, higher AC, and lower DEN than other lava flows, as well as a jagged shape due to the internal structure.

3.3 Identification of intermediate mafic lava architecture

The intermediate mafic lava has the characteristics of a wide flow range and multiple eruption units that interlace and overlap. For example, the basalt lava flow of the Faroe Islands extends at least

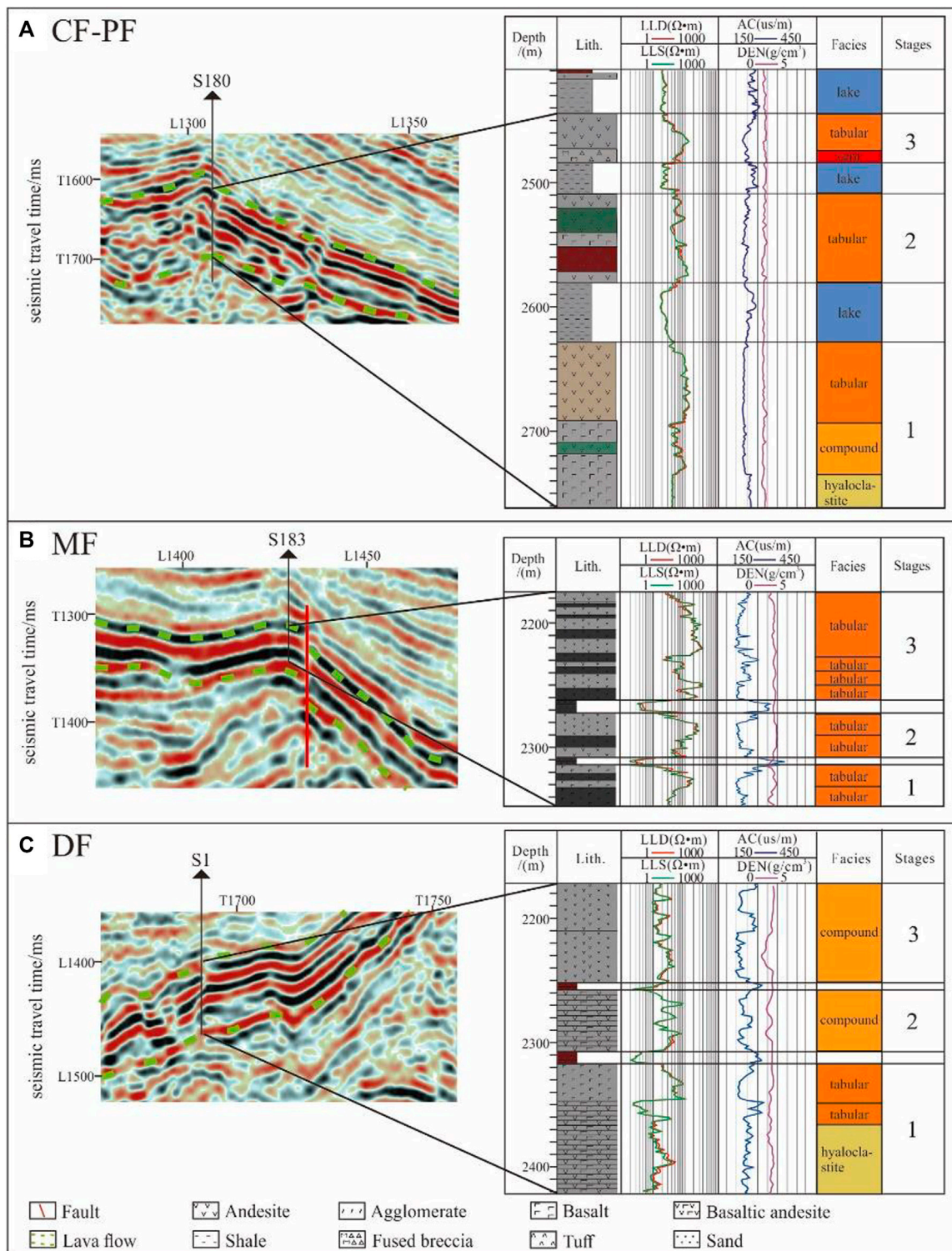


FIGURE 5 Conventional logging response of different lava flows in CF-PF (A), MF (B) and DF (C), respectively. LLD, Deep lateral resistivity logging, LLS, Shallow resistivity logging, AC, Acoustic logging, DEN, Density logging.

6.6 km (Jerram et al., 2009). Intermediate mafic volcanoes may be affected by the superimposition of other volcanic lavas, which makes it impossible to reflect the distribution characteristics of volcanic craters according to the thickness and scale of the lava flows.

Well S180 showed basaltic agglomerated lava 2480 m in depth. The core showed a breccia structure. Observation of the core showed that the size of the blasted breccia was uneven. The seismic profile showed that the volcanic channel formed along the fault near the

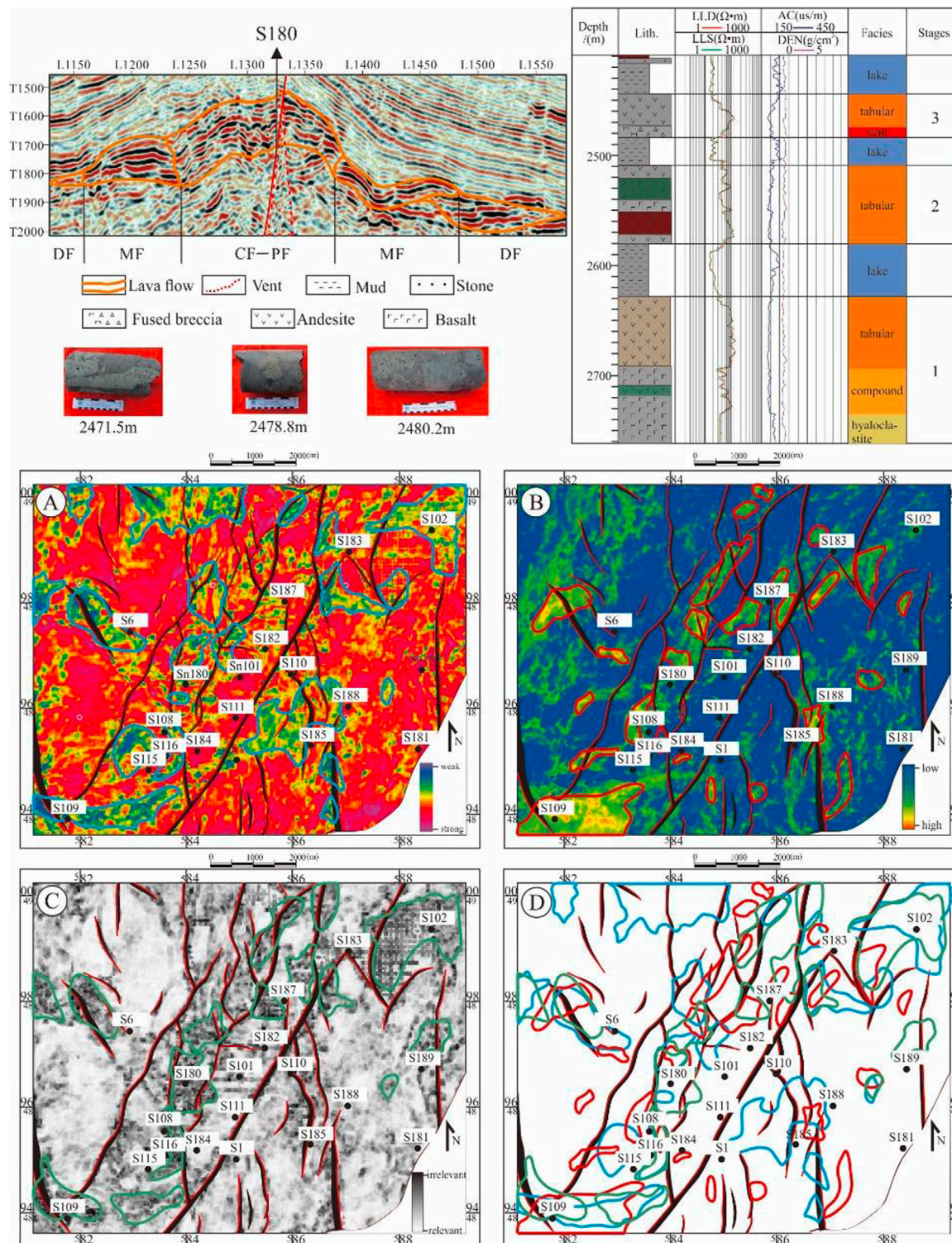


FIGURE 6 Identification of craters through core, well logging, and seismic attributions. (A) Root mean square (RMS) amplitude. Blue circles, craters. (B) Stratigraphical dip attribution. Red circles, craters. (C) Coherence attribution. Green circles, craters. (D) Combination of the three methods to identify craters.

drilling well, which was characterized by time-lapse, poor stratigraphic continuity, medium weak amplitude, and high dip angle (Figure 6). Crater identification is an important factor in the

description of volcanic architecture. Based on the seismic response characteristics, the distribution of craters was characterized according to amplitude, dip angle, and coherence, respectively.

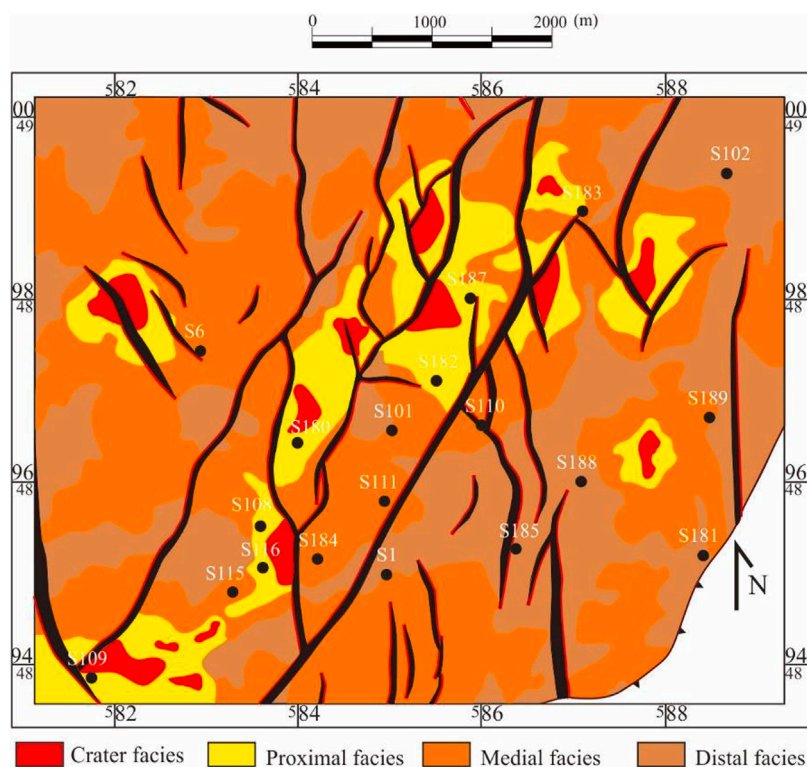


FIGURE 7
Distributions of the facies zones of intermediate mafic lava flows.

Finally, the distribution of craters was determined based on the combination of the aforementioned three attributes (Figure 6). The distribution of volcano craters showed that most intermediate mafic volcanoes were formed by the progress of the lava overflow through the faults, especially at crossing faults.

According to the volcanic seismic facies characteristics of well S180, the volcanic architecture can be divided into CF-PF, MF, and DF. The seismic response characteristics of CF-PF included a weak root mean square amplitude, high dip angle, and poor coherence. The seismic response characteristics of the MF were a strong root mean square amplitude and good correlation. The seismic response characteristics of the DF were weak root mean square amplitude, poor correlation, and small dip angle (Figure 6). The distributions of the facies zone of intermediate mafic lava flows are shown in Figure 7.

4 Discussion

4.1 Formation mechanisms of the reservoirs

The volatile gas content of mafic magma is relatively high, and the magma temperature can reach $>1,100^{\circ}\text{C}$ (Iio et al., 2018). During overflow along the surface after magma eruption, gas escapes and forms many vesicles under the dual effects of temperature and pressure (He et al., 2019). Due to the instability of plagioclase and other mafic minerals in the mafic lava, alteration is easy to occur in the presence of fluid (Figure 8E). Different types of secondary minerals, mainly calcite and chlorite, fill the vesicles and form the amygdalites (Figures 8A, D, F).

These may originate from the precipitation of iron and calcium ions during the dissolution of intermediate mafic lava, providing a material basis for the formation of calcite and chlorite in the open spatial pores and fissures. Volcanic eruptions are greatly affected by tectonic activities (Li et al., 2022). Volcanic institutions are mostly distributed near faults, and structural fissures of different sizes can be observed at the core (Figure 8I). Basaltic agglomerated lava develops blast cracks filled with mafic magma liquid (Figure 8H). In addition to primary pores and fissures, the main reservoir space of natural gas is secondarily dissolved pores and fissures, including mineral-dissolved pores, filling-dissolved pores, and some glassy devitrification pores (Figures 8C, G). The minerals on the edge of the vesicles are prone to chloritization due to their contact with the fluid (a chlorite ring around the vesicle is visible in Figures 8A, B).

4.2 Reservoir geological model

The energy of fissure overflow-type mafic volcanoes is weak in the initial stage of eruption. The volcanic eruption gradually increases with the upwelling of volatile gas before later decreasing (Ni et al., 2014). A lava flow is rich in volatiles near the volcano crater, mostly porous lava, lava with foam structure, and welded breccia. The upper part of the tabular lava flow is mainly distributed with a large pore zone; the volatile escapes upward, the middle part forms a dense block, and the columnar joint develops after condensation and contraction (Walker et al., 1971). Volatiles that cannot easily escape remain at the bottom, forming a sparse

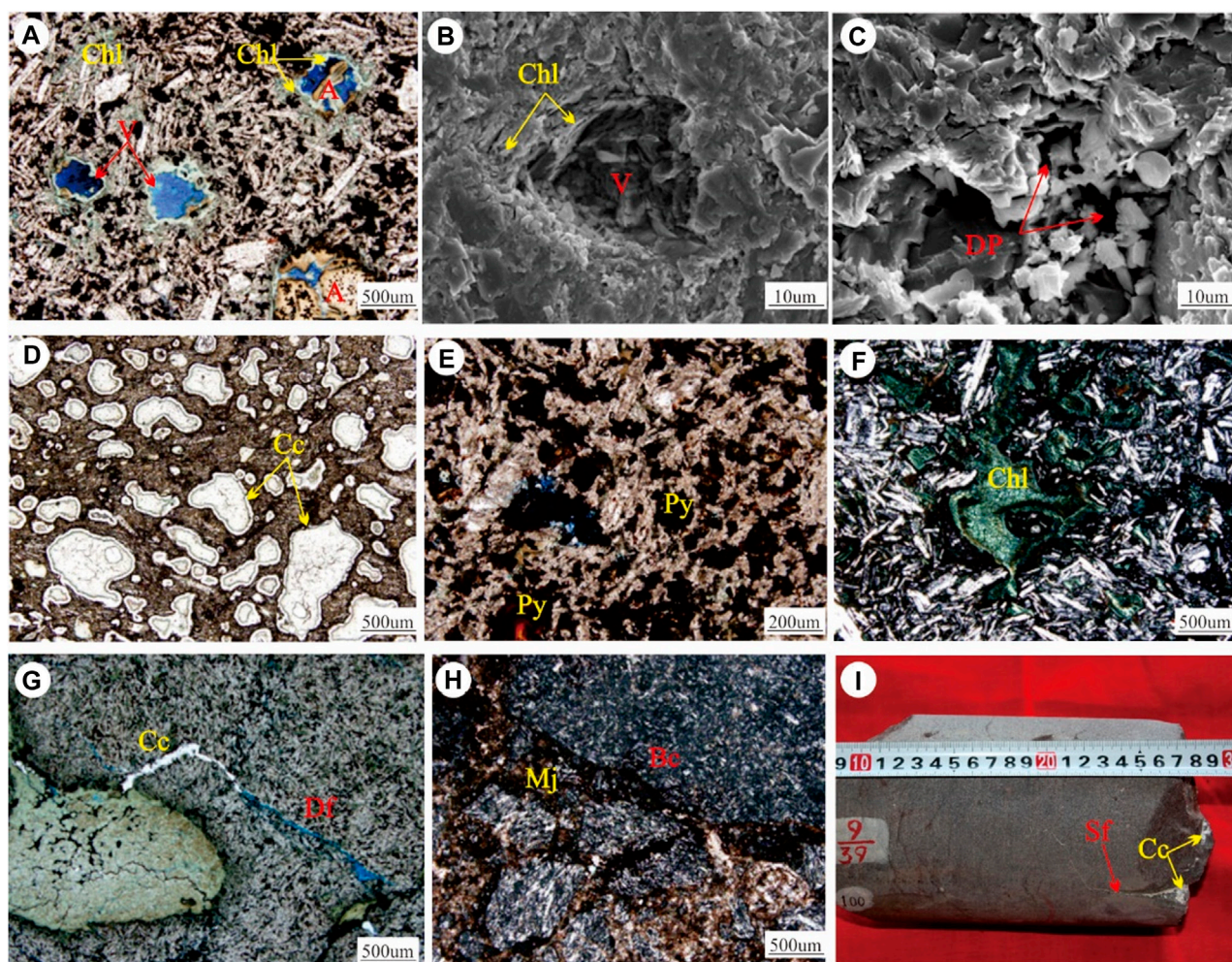


FIGURE 8

Space types of intermediate mafic lava reservoirs in the Yingcheng Formation of the Changling fault depression. (A) S116 well, 2,714.2 m, basalt, vesicle, and amygdale development. (B) S116 well, 2,715.2 m, basalt, micron vesicle. (C) S1 well, 2,403.3 m, andesite, dissolved pores. (D) S116 well, basalt, vesicle filled with calcite. (E) S102 well, 1857.1 m, basalt, mafic minerals. (F) S180 well, 2,471.5 m, basaltic andesite, chlorite-filled pores, and chloritization of some mafic minerals. (G) S1 well, 2,402 m, andesite, fissure filled with calcite and dissolution. (H) S180 well, 2,480.2 m, basaltic agglomerated lava, mafic magma juice filling the blast crack. (I) S187 well, 2,436.1 m, basalt, structural fissures filled with calcite. V, vesicle; Dp, dissolved pore; A, amygdale; Df, dissolved fissure; Bc, blast crack; Sf, structural fissure; Cc, calcite; Chl, chlorite; Py, pyroxene; Mj, mafic magma juice.

pore zone with small pores. The erupted magma flows from the crater to far distances, which in the MF is relatively dense and thick, with some sparse and smaller pores on the lava flow surface. The internal structure characteristics of single lava flows are the same as those of near-source lava flows, with upper pore zones, middle dense zones, and lower sparse pore zones. The thin-layer lava flow in the DF is interlaced and overlapped. The volatile content in DF is low, and the pores are very small. The facies architecture shows two situations of hyaloclastite were formed by magma quenching in water. One is volcanic eruption at the bottom of the lake, which formed near the bottom of the crater; the other is onshore eruption, in which the lava flowed into the lake at the distal end to form. The hyaloclastite recrystallized to form devitrification pores (Zhao et al., 2009). Based on the aforementioned understanding of the morphology, occurrence, and lithofacies combination characteristics of different facies belts of volcanic institutions, and the internal structure of the intermediate mafic lava flows unit, the

lithofacies model of the intermediate mafic lava flows is established (Figure 9).

4.3 Relationships between reservoir physical characteristics and facies architecture

The volcanic lava in the study area is a low-porosity and ultra-low permeability reservoir, in which the physical properties of the reservoir in different facies zones vary greatly (Figure 10). The porosity distribution of the CF-PF ranges from 3% to 14%, the average porosity of the top vesicle zone is as high as 12.4%, and the permeability is approximately 1 mD. This is the main target area for oil and gas exploration. According to the mercury injection curve characteristics of the rock samples, the maximum mercury injection saturation of rock samples reached 80%, further indicating the high reservoir porosity and good connectivity. The rising section of the

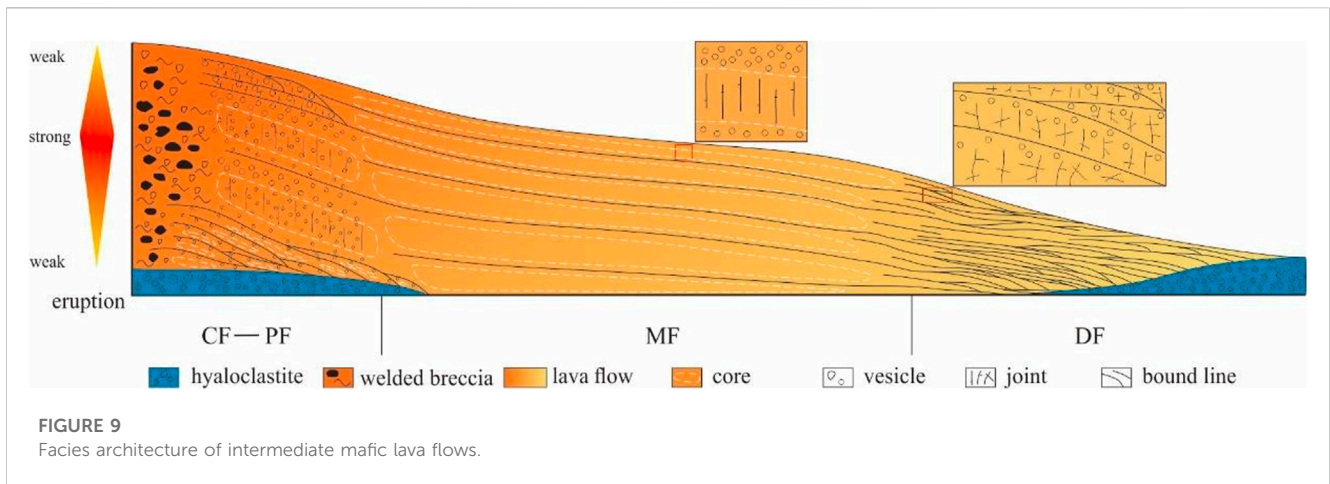


FIGURE 9
Facies architecture of intermediate mafic lava flows.

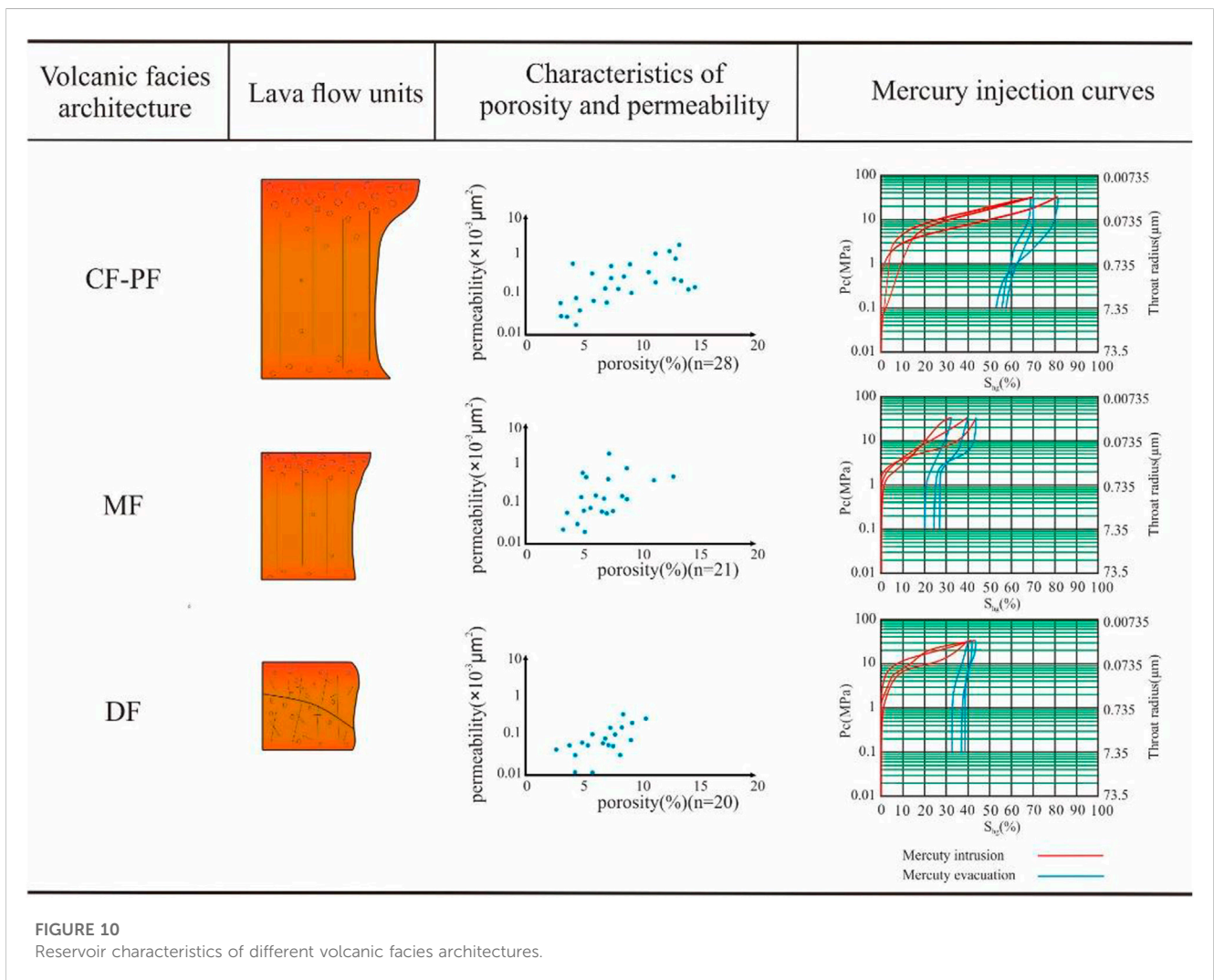


FIGURE 10
Reservoir characteristics of different volcanic facies architectures.

mercury injection curve shows the presence of micro-sized pores in the rock samples. The porosity of the reservoir in the MF was mostly distributed between 5% and 8% and the permeability was <1 mD. The mercury injection curve showed strong heterogeneity, with a mercury

injection saturation of <40%. Moreover, the connectivity of the pores and fractures was not good, which verified the characteristics of small pores and micro-fractures, consistent with the lava flow structure of the original facies zone. The reservoir porosity and permeability

characteristics of the DF were similar to those of the MF. The mercury injection curve was characterized by nano-pores, a low maximum mercury injection saturation, and a mercury removal rate far lower than those of other facies zones, which further indicated the poor connectivity of its reservoir space. The reservoir space of the DF may be mainly composed of dissolution micropores and devitrification pores.

5 Conclusion

- 1) Intermediate mafic lava flows can be divided into tabular lava flow, compound lava flow, and hyaloclastite, which can be identified by seismic attributes such as seismic profile morphology (parallel, sub-parallel, braided, or pillow-shaped), amplitude (strong, medium, or weak), and frequency (high, medium, or low), and can also be identified by logging response characteristics (resistivity, AC, and DEN).
- 2) Craters characterized by time-lapse showed poor stratigraphic continuity, medium-weak amplitude, and high dip angle, which is one important factor in the description of volcanic architecture. The facies architectures consisted of CF-PF, MF, and DF (far away from the crater). The seismic response characteristics of the CF-PF included a weak root mean square amplitude, high dip angle, and poor coherence. The MF showed a strong root mean square amplitude and good correlation, while the DF showed a weak root mean square amplitude, poor correlation, and small dip angle.
- 3) The types of reservoir space were mainly vesicles, amygdale inner pores, dissolved pores, devitrification pores, and other fissures. Compared with other volcanic rocks, the alteration of mafic minerals is an important factor leading to secondary mineral filling. The physical properties of intermediate mafic lava reservoir mainly depended on three factors, namely, primary pore development, secondary mineral filling, and dissolution.
- 4) Comparison of the gas physical property analyses and the mercury intrusion curve characteristics showed that the porosity and permeability of the CF-PF were higher than those of the MF and DF, the proportion of micro-scale pores was relatively high, and the pore connectivity was the best, especially the top vesicle zone, in the CF-PF, with porosity as high as 12.4%, and permeability of approximately 1 mD, making it the main target area for oil and gas exploration.

References

- Angulo-Preckler, C., Pernet, P., García-Hernández, H., Kereszturi, G., Álvarez-Valero, A. M., Hopfenblatt, J., et al. (2021). Volcanism and rapid sedimentation affect the benthic communities of Deception Island, Antarctica. *Cont. Shelf Res.* 220 (71), 104404. doi:10.1016/j.csr.2021.104404
- Byrnes, R., and Jeffrey, M. (2002). Morphology, stratigraphy, and surface roughness properties of Venusian lava flow fields. *J. Geophys. Res.* 107 (10), 5079. doi:10.1029/2001je001828
- Cang, Z., Shan, X., Yi, J., Yue, Q., Xu, C., Zou, X., et al. (2021). Fractal characterization of nanoscale pores of volcanic reservoirs in the Dongling area, Changling fault depression, Songliao Basin. *Nat. Resour. Res.* 30, 3483–3502. doi:10.1007/S11053-021-09867-9
- Caroff, M. (2019). Emplacement of lobate sheet flows with hyaloclastites onto soft sediment: The Erquy Neoproterozoic lava pile, Armorican Massif (France). *Precambrian Res.* 334, 105454. doi:10.1016/j.precamres.2019.105454
- Clague, D., Moore, J., and Alicé, S. (2013). *Volcanic breccia and hyaloclastite in blocks from the nuuanu and wailau landslides*. Hawaii: American Geophysical Union AGU.
- Fan, C., Qin, Q., Lou, X., Pretorius, D., and Menasche, P. (2020). Formation mechanisms and distribution of weathered volcanic reservoirs: A case study of the carboniferous volcanic rocks in northwest Junggar Basin, China. *Energy Sci. Eng.* 8 (8), 1–10. doi:10.1016/j.yjmcc.2020.03.003
- Feng, Z., Yin, C., Liu, J., Zhu, Y., Lu, J., and Li, J. (2014). Formation mechanism of *in-situ* volcanic reservoirs in eastern China: A case study from xushen gasfield in Songliao Basin. *Sci. China Earth Sci.* 57 (12), 2998–3014. doi:10.1007/s11430-014-4969-2
- Greeley, R. (1982). The snake river plain, Idaho: Representative of a new category of volcanism. *J. Geophys. Res.* 87 (B4), 2705–2712. doi:10.1029/JB087iB04p02705
- Hachimi, H., Youbi, N., and Madeira, J. (2010). "Morphology and emplacement mechanisms of the lava flows of the central atlantic magmatic province (CAMP) of Morocco," in *II central and north atlantic conjugate margins conference*. Editors R. Pena dos Reis and N. Pimentel (Lisbon, Portugal: Rediscovering the Atlantic: New ideas for an old sea). doi:10.1144/SP357.9

Data availability statement

The original contributions presented in the study are included in the article/Supplementary Material. Further inquiries can be directed to the corresponding author.

Author contributions

Software, ZC and JH; investigation, BW and HW; data curation, XR; writing—original draft, QY; writing—review and editing, CL; visualization, RZ. All authors have read and agreed to the published version of the manuscript.

Funding

This research was funded by financial support from the Educational Department of Liaoning Province (grant numbers LJKZ0392, LJKZ0394, and L2020047) and a Liaoning Marine Economy Development Project (grant number HYZX202110).

Conflict of interest

Author ZC was employed by the Chengdu Exploration and Development Research Institute of Petro China Daqing Oilfield Company Ltd., China. Authors XR and JH were employed by the Northeast Oil & Gas Branch of Sinopec.

The remaining authors declare that the research was conducted in the absence of any commercial or financial relationships that could be construed as a potential conflict of interest.

Publisher's note

All claims expressed in this article are solely those of the authors and do not necessarily represent those of their affiliated organizations, or those of the publisher, the editors, and the reviewers. Any product that may be evaluated in this article, or claim that may be made by its manufacturer, is not guaranteed or endorsed by the publisher.

- He, Q., Li, Y., and She, S. (2019). Mechanical properties of basalt specimens under combined compression and shear loading at low strain rates. *Rock Mech. Rock Eng.* 52, 4101–4112. doi:10.1007/s00603-019-01806-8
- Hou, L., Luo, X., Wang, J., Yang, F., Zhao, X., and Mao, Z. (2013). Weathered volcanic crust and its petroleum geological significance: A case study of the carboniferous volcanic crust in northern xinjiang, NW China. *Petroleum Explor. Dev.* 40 (7), 277–286. doi:10.1016/S1876-3804(13)60034-8
- Huang, Y., Wang, P., Shu, P., Xu, C., Lu, X., Zhang, W., et al. (2010). Avian influenza virus and Newcastle disease virus (NDV) surveillance in commercial breeding farm in China and the characterization of Class I NDV isolates. *Acta Petrol. Sin.* 26 (1), 82–86. doi:10.1016/j.petrol.2010.01.003
- Iio, Y., Sibson, R., Takeshita, T., Sagiya, T., Shibazaki, B., and Nakajima, T. J. (2018). Crustal dynamics: Unified understanding of geodynamic processes at different time and length scales. *Earth Planets Space* 70 (1), 97. doi:10.1186/s40623-018-0869-6
- Jerram, D., Single, R., Hobbs, R., and Nelson, C. E. (2009). Understanding the offshore flood basalt sequence using onshore volcanic facies analogues: An example from the faroe–shetland basin. *Geol. Mag.* 146 (3), 353–367. doi:10.1017/S0016756809005974
- Li, H., Qin, Q. R., Zhang, B. J., Ge, X. Y., Hu, X., Fan, C. H., et al. (2020). Tectonic fracture formation and distribution in ultradeep marine carbonate gas reservoirs: A case study of the maokou Formation in the jiulongshan gas field, sichuan basin, southwest China. *Energy and Fuels* 34, 14132–14146. doi:10.1021/acs.energyfuels.0c03327
- Li, H., Tang, H. M., Qin, Q. R., Zhou, J. L., Qin, Z. J., Fan, C. H., et al. (2019). Characteristics, formation periods and genetic mechanisms of tectonic fractures in the tight gas sandstones reservoir: A case study of xujiahe Formation in YB area, sichuan basin, China. *J. Petroleum Sci. Eng.* 178, 723–735. doi:10.1016/j.petrol.2019.04.007
- Li, H., Zhou, J., Mou, X., Guo, H., and Wang, X. (2022). Pore structure and fractal characteristics of the marine shale of the longmaxi Formation in the changling area, southern sichuan basin, China. *Front. Earth Sci.* 10, 1018274. doi:10.3389/FEART.2022.1018274
- Li, J., Li, H., Yang, C., Ren, X. H., and Li, Y. D. (2023). Geological characteristics of deep shale gas and their effects on shale fracability in the Wufeng–Longmaxi Formations of the southern Sichuan Basin, China. *Lithosphere* (1), 4936993. doi:10.2113/1970/4936993
- Liu, W., Huang, Y., and Pang, Y. (2010). Diagenesis of intermediate and mafic volcanic rocks of Yingcheng Formation (K1y) in the Songliao Basin: Sequential crystallization, amygdale filling and reservoir effect. *Acta Petrol. Sin.* 26 (1), 158–164. doi:10.1000-0569/2010/026(01)-0158-64
- Marsh, J., Ewart, A., Milner, S., Duncan, A., and Miller, R. (2001). The etendeka igneous Province: Magma types and their stratigraphic distribution with implications for the evolution of the paraná-etendeka flood basalt province. *Bull. Volcanol.* 62 (6-7), 464–486. doi:10.1007/s004450000115
- Nelson, C., Jerram, D., and Hobbs, R. (2009). Flood basalt facies from borehole data: Implications for prospectivity and volcanology in volcanic rifted margins. *Pet. Geosci.* 15 (4), 313–324. doi:10.1144/1354-079309-842
- Ni, H., Keppler, H., Walte, N., Schiavi, F., Chen, Y., Masotta, M., et al. (2014). *In situ* observation of crystal growth in a basalt melt and the development of crystal size distribution in igneous rocks. *Contributions Mineralogy Petrology* 167 (5), 1003–1013. doi:10.1007/s00410-014-1003-9
- Nichols, A., Potuzak, M., and Dingwell, D. (2012). Cooling rates of basaltic hyaloclastites and pillow lava glasses from the HSDP2 drill core. *Geochimica Cosmochimica Acta* 73 (4), 1052–1066. doi:10.1016/j.gca.2008.11.023
- Passey, S., and Bell, B. (2007). Morphologies and emplacement mechanisms of the lava flows of the Faroe Islands basalt group, Faroe Islands, NE atlantic ocean. *Bull. Volcano* 70 (2), 139–156. doi:10.1007/s00445-007-0125-6
- Ren, J., Tamaki, K., Li, S., and Junxia, Z. (2022). Late Mesozoic and Cenozoic rifting and its dynamic setting in Eastern China and adjacent areas. *Tectonophysics* 344 (3-4), 175–205. doi:10.1016/S0040-1951(01)00271-2
- Ren, X., Shan, X., and Yi, J. (2017). Characteristics and quantitative evaluation of reservoir in lava flow units in the early cretaceous Yingcheng Formation in changling depression of Songliao Basin. *J. China Univ. Petroleum Ed. Nat. Sci.* 41 (5), 30–40. doi:10.3969/j.issn.1673-5005.2017.05.004
- Self, S., Thordarson, T., and Keszthelyi, L. (2013). Emplacement of continental flood basalt lava flows. *Geophys. Monogr. Ser.*, 381–410.
- Shan, S. C., Wu, Y. Z., Fu, Y. K., and Zhou, P. H. (2021). Shear mechanical properties of anchored rock mass under impact load. *J. Min. Strata Control Eng.* 3 (4), 043034. doi:10.13532/j.jmsce.cn10-1638/td.20211014.001
- Shan, X., Gao, X., and Xu, H. (2012). The main factors of intermediate and mafic volcanic gas reservoir forming of Yingcheng Formation in Anda Area of Songliao Basin. *J. Jilin Univ. (Earth Sci. Ed.)* 42 (5), 1348–1357.
- Single, R., and Jerram, D. (2004). The 3D facies architecture of flood basalt provinces and their internal heterogeneity: Examples from the palaeogene skye lava field. *J. Geol. Soc.* 161 (6), 911–926. doi:10.1144/0016-764903-136
- Tang, H., Pang, Y., and Bian, W. (2008). Quantitative analysis on reservoirs in volcanic edifice of early cretaceous Yingcheng Formation in Songliao Basin. *Acta Pet. Sin.* 29 (6), 841–845.
- Tang, H., Wang, L., Wu, H., Hu, J., Dai, X., Goh, T. L., et al. (2023). Possible geological interpretation of the volcanic seismic facies based on volcanostratigraphy elements: A case analysis of the Yingcheng Formation in the Changling fault depression, Songliao Basin, ne China. *Geoenergy Sci. Eng.* 225, 211668. doi:10.1016/j.geoen.2023.211668
- Walker, G. (1993). Basaltic-volcano systems. *Geol. Soc. Lond. Spec. Publ.* 76 (1), 3–38. doi:10.1144/GSL.SP.1993.076.01.01
- Walker, G. (1971). Compound and simple lava flows and flood basalts. *Bull. Volcanol.* 35 (3), 579–590. doi:10.1007/BF02596829
- Wang, J., Jin, J., Zhu, R., Rabkin, S. D., and Liu, R. (2011). Oncolytic herpes simplex virus treatment of metastatic breast cancer. *Acta Pet. Sin.* 32 (5), 757–763. doi:10.3892/ijo.2011.1266
- Wang, P., and Chen, S. (2015). Cretaceous volcanic reservoirs and their exploration in the Songliao Basin, northeast China. *AAPG Bull.* 99 (3), 499–523. doi:10.1306/09041413095
- Wang, P., He, K., and Yi, J. (2018). Volcanostratigraphy, volcanic architecture and reservoir of intermediate-mafic volcanic rocks: A comparison between buried cretaceous volcanoes in the Songliao Basin and the modern volcanoes in changbai mountain. *Acta Pet. Sin.* 57 (5), 775–787. doi:10.3969/j.issn.1000-1441.2018.05.017
- Wei, H., Liu, J., and Meng, Q. (2010). Structural and sedimentary evolution of the southern Songliao Basin, northeast China, and implications for hydrocarbon prospectivity. *AAPG Bull.* 94 (4), 533–566. doi:10.1306/09080909060
- Yi, J., Tang, H., and Wang, P. (2016). Types, characteristics and reservoir significance of basic lava flow units. *J. Central South Univ. Sci. Technol.* 47 (1), 149–158. doi:10.11817/j.issn.1672-7207.2016.01.022
- Yue, Q., Shan, X., Zhang, X., Xu, C., Yi, J., and Fu, M. (2021). Quantitative characterization, classification, and influencing factors of the full range of pores in weathering crust volcanic reservoirs: Case study in bohai Bay basin, China. *Nat. Resour. Res.* 30, 1347–1365. doi:10.1007/s11053-020-09774-5
- Zhang, C., Wu, C., and Xie, L. (2012). Filling characteristics and evolution analysis of the early Cretaceous small fault depression in Dongling region, Songliao Basin. *Acta Sci. Nat. Univ. Pekin.* 48 (2), 253–261. doi:10.13209/j.0479-8023.2012.034
- Zhang, X., Xia, Y., Zhang, Y., Chen, Y., Zhang, G., and Gao, W. (2018). Volcanic reservoir characteristics and hydrocarbon Genesis of Jiamuhe formation in Jinlong 2 wellblock, Junggar Basin. *Petroleum Sci. Technol.* 36 (19), 1516–1523. doi:10.1080/10916466.2018.1471486
- Zhao, H., Huang, W., and Wang, C. (2009a). Micropores from devitrification in volcanic rocks and their contribution to reservoirs. *Oil Gas. Geol.* 30 (1), 47–58.
- Zhao, W., Zou, C., Li, J., Feng, Z., Zhang, G., Hu, S., et al. (2009b). Comparative study on volcanic hydrocarbon accumulations in Western and eastern China and its significance. *Petroleum Explor. Dev.* 36 (1), 1–11. doi:10.1016/S1876-3804(09)60106-3
- Zou, C., Zhao, W., Jia, C., Zhu, R. K., Zhang, G. Y., Zhao, X., et al. (2008). Formation and distribution of volcanic hydrocarbon reservoirs in sedimentary basins of China. *Petroleum Explor. Dev.* 35 (3), 257–271. doi:10.1016/S1876-3804(08)60071-3